IHJPAS. 37 (2) 2024
Ibn Al-Haitham Journal for Pure and Applied Sciences
Journal homepage: jih.uobaghdad.edu.iq
PISSN: 1609-4042, EISSN: 2521-3407

Synthesis and Spectral Study of New Guanine Derivative (N-((6-Oxo-6,9-Dihydro-1*H*-Purin-2-yl)Carbamothioyl)Propionamide) and its Complexes with Some Metals Ion

Abdullah Sh. Abdullah Alani[1*], Basima Muhsen Sarhan[2] and Vishwa Deepak Tripathi[3]

[1]Directorate of Institutional Development and Government Coordination, Iraqi Ministry of Education, Baghdad, Iraq.
[2]Department of Chemistry, College of Education for Pure Science (Ibn Al–Haitham), University of Baghdad, Baghdad, Iraq.
[3]Department of Chemstry, C.M. Science College, Lalit Narayan Mithila University, Darbhanga, Bihar, India.

*Corresponding Author.

Received: 6 March 2023 Accepted: 23 May 2023 Published: 20 April 2024

doi.org/10.30526/37.2.3313

Abstract

This study included the preparation and characterization of the new guanine derivative (N-((6-oxo-6,9-dihydro-1H-purin-2-yl)carbamothioyl)propionamide), with an exciting chemical structure. The guanine part is a bicyclic heterocyclic base that is connected to a carbamothioyl group by a propionamide linker. This nitrogenous base derivative is prepared in two steps: The first step involves the synthesis of propionyl isothiocyanate from the reaction of propionyl chloride with ammonium thiocyanate in acetone. In contrast, the second step consists of the reaction of ammonium thiocyanate with guanine to obtain the ligand. The study also includes the preparation of new complexes of metal ions (Mn^{+2}, Co^{+2}, Ni^{+2}, Cu^{+2}, Zn^{+2}, Cd^{+2}, and Pd^{+2}) with a prepared guanine derivative. The ligand and complexes were characterized by using infrared spectra, ultraviolet-visible spectra, ^{1}H-N.M.R., ^{13}C-N.M.R. spectra, and elemental analysis (C.H.N.S.): molar conductivity measurement, magnetic susceptibility, atomic absorption, and melting point. The results of these studies showed that general formulas for these complexes were given $[MCl_2(O.P.P.)_2]$, M = (Mn^{+2}, Co^{+2}, Ni^{+2}, Cu^{+2}, Zn^{+2}, Cd^{+2}, and Pd^{+2}). It was found that the geometric shape of all the prepared complexes was an octahedron.

Keywords: Guanine, propionyl chloride, isothiocyanate, coordination complexes, organometallic compounds.

1. Introduction

Bioinorganic chemistry is a field of chemistry that focuses on the study of the interactions between inorganic molecules and biological systems. It involves the study of metal ions and their coordination chemistry in biological systems, as well as the role of inorganic elements and compounds in biological processes [1,2].

The preparation of metallic coordination complexes with biological molecules is an active area of research in bioinorganic chemistry because these complexes can have a variety of biological applications. For example, some of these complexes have been studied for their potential use as anticancer agents, antibacterials, antifungals, or catalysts for important biological reactions [3–10].

The preparation of these complexes often involves modifying the biological molecules to create ligands that can coordinate with metal ions and form stable complexes [3,10–14]. This can affect the use of synthetic organic chemistry techniques to develop modified versions of naturally occurring biological molecules or the development of entirely new ligands that can alter the properties of biological molecules [4,15–17].

The objective of this study is to synthesize and analyze the properties of a novel ligand (OPP) (N-((6-oxo-6,9-dihydro-1H-purin-2-yl)carbamothioyl)propionamide), and its complexes with some metal ions.

2. Materials and Methods

2.1 Chemicals

All reagents, chemicals, metal chloride salts, and solvents were purchased from Merck, Fluorochem, Fluka, Sigma-Aldrich, J.T. Baker, BDH, Riedel-De Haen Merk, and Honeywell with high purity.

2.2 Synthesis of the ligand (OPP)

A- About 30 mmol, 2.28 g of ammonium thiocyanate was dissolved in 20 mL of acetone with stirring, then 30 mmol, 2.77 mL of propionyl chloride was added to the solution and stirred for about 3 hours, then filter. The product was a yellow solution.

B- About 30 mmol, 4.53 g of guanine was dissolved in 20 mL of acetone, then mixed with the former solution above, refluxed the mixture with a water bath for 6 hours, let dry, and then recrystallized with ethanol [18,19], as in **Scheme 1**.

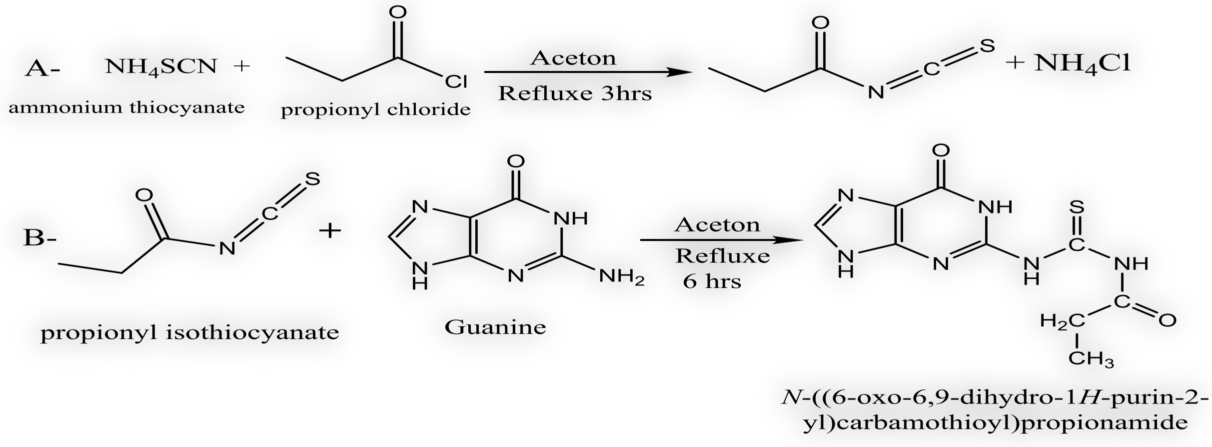

Scheme1. Preparation of ligand (OPP).

The product was orange gummy, yield (63%), m.p (134°C), C% found (40.48) calc.(40.60), H% was found (3.47) calc.(3.79), N% was found (31.33) calc.(31.56), S% was found (12.39) calc.(12.04), and O% was found (12.39) calc.(12.02).

2.3 Synthesis of metal complexes

A- About 2 mmol, 0.532 g of the guanine derivative was dissolved in 10 mL of ethanol.

B- About 1 mmol of the metal salts (0.197 g of $MnCl_2.4H_2O$, 0.237 g of $CoCl_2.6H_2O$, 0.237 g of $NiCl_2.6H_2O$, 0.170 g of $CuCl_2.2H_2O$, 0.136g of $ZnCl_2$, 0.201 g of $CdCl_2.H_2O$, and 0.177 g of $PdCl_2.H_2O$) were dissolved in the least amount of ethanol, then this solution was added to the solution obtained from the previous step and the mixture stirred for 4 hours to form a precipitate that is separated by filtration, washed with ethanol, and leave to dry [19,20]. **Table 1** shows some physical properties of the prepared complexes.

3. Results and Discussion

The solid complexes that were synthesized displayed solubility in certain typical solvents, including dimethyl formamide and dimethyl sulphoxide, and exhibited considerable thermal stability. When dissolved in DMSO, all complexes demonstrated non-electrolytic behavior, as evidenced by their molar conductivity. **Table 1** shows the percentage of physical properties and metals in complexes and the molar conductivity of the ligand and its metallic complexes.

Table 1. The physical properties of the ligand and its metallic complexes.

Compound	Color	M.Wt (g/mol)	M.p.(Dec.) °C	M% Calculation (Found)	Molar condu. $Ohm^{-1}cm^{2}mol^{-1}$
(OPP)	Orange	266.28	134	-- (--)	---
$[MnCl_2(OPP)_2]$	Yellow	658.40	142	8.34 (8.58)	14
$[CoCl_2(OPP)_2]$	Blue	662.39	164	9.80 (9.72)	12
$[NiCl_2(OPP)_2]$	Green	662.15	168	8.86 (9.01)	18
$[CuCl_2(OPP)_2]$	Blue	667.00	--- (182)	9.53 (9.77)	12
$[ZnCl_2(OPP)_2]$	White	688.84	--- (168)	9.78 (9.72)	10
$[CdCl_2(OPP)_2]$	White	715.87	--- (192)	15.70 (15.83)	8
$[PdCl_2(OPP)_2]$	Brown	709.88	--- (188)	14.99 (15.08)	2

The FT-IR spectrum for free ligand OPP in **Figure 1**, detected a medium band at (3160 cm^{-1}) for υ(NH), medium band at (1604 cm^{-1}) for υ(C=O amidic) and another bands at (1226 cm^{-1}) for υ(C=S) and a strong band at (1695 cm^{-1}) for υ(C=O) of the guanine ring [22], **Table 2** and **Figure 1**.

Table 2. The FT-IR bands for guanine and free ligand OPP.

Compound	ν($N-H_2$+OH)	ν(N-H+OH)	ν(C=O) Amide	ν(C=S)	ν(C=O) in purin ring
Guanine	$3321_{(m)}$	$3116_{(m)}$	---	---	$1693_{(s)}$
OPP	-----	$3160_{(m)}$	$1604_{(s)}$	$1226_{(s)}$	$1695_{(s)}$

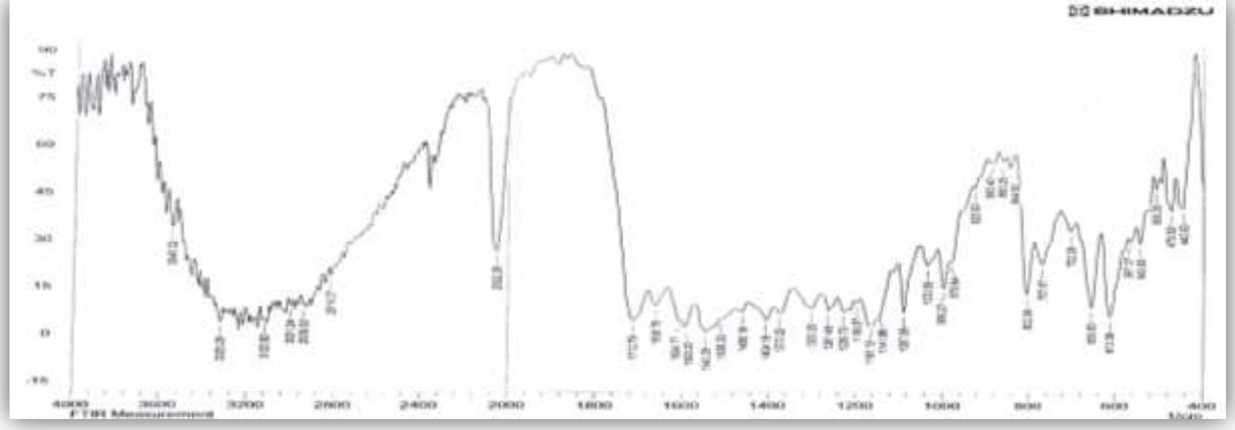

Figure 1. The FT-IR spectrum of ligand (OPP).

The ^{1}H-NMR spectrum of ligand (OPP) in DMSO-d_6 in **Figure 3** showed a doublet signal at δ(1.03) ppm for (3H, of CH_3 methyl), a pentet signal at δ(2.145) ppm for two protons in (CH_2, methylene), a single signal at δ(2.51) ppm for (DMSO), a single signal at δ(7.02) ppm for one proton of (N-H imidazole ring), a single signal at δ(7.28) ppm for one proton (C-H in imidazole ring), a single signal at δ(9.34) ppm for one proton of (NH, amine), a single signal at δ(9.64) ppm for one proton in (NH, amide). Also, a single signal at δ(11.048) ppm for one proton in (NH, guanidine) [22], **Table 2**.

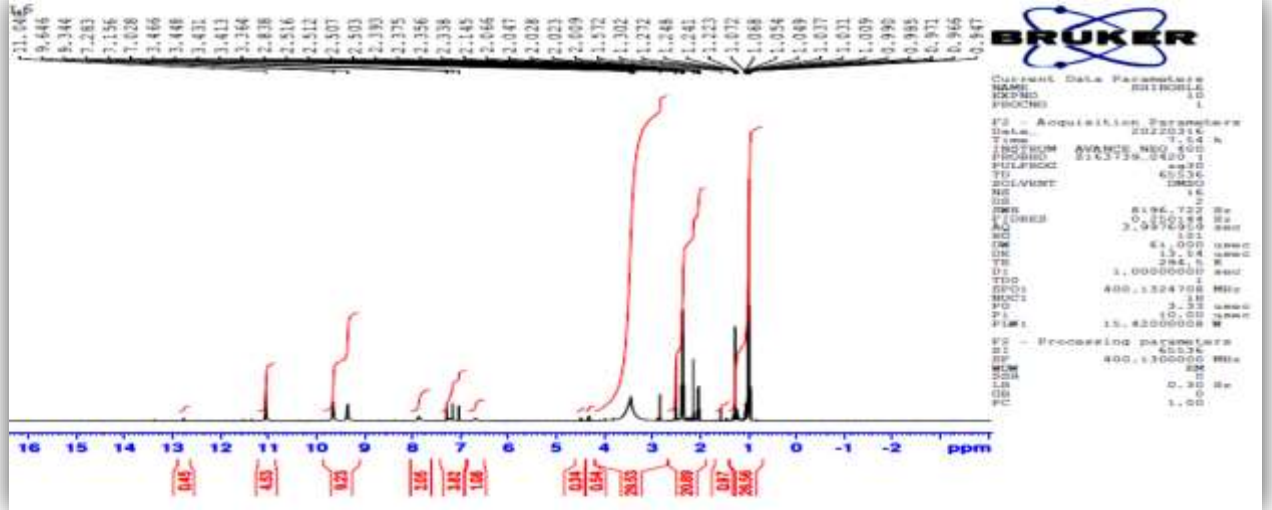

Figure 2. The ^{1}H-NMR spectrum of ligand (OPP).

Table 3. The ^{1}HNMR signals for ligand (OPP).

Symbol	Δppm	Signal	No.of point	Group
a	1.03	Doublet	3H	CH_3, Methyl
b	2.145	Pentlet	2H	CH_2, Methylene
c	7.02	Singlet	1H	N-H, imidazole ring
d	7.28	Singlet	1H	C-H, imidazole ring
e	9.34	Singlet	1H	N-H, amine
f	9.64	Singlet	1H	N-H, amide
g	11.04	Singlet	1H	N-H, guanidine

While the ^{13}C-NMR spectrum of ligand OPP in **Figure 4**, DMSO-d_6 showed a single signal at $\delta(10.23)$ ppm for (CH_3, methyl), a single signal at $\delta(30.02)$ ppm for (CH_2 methylene), a single signal between $\delta(39.31\text{-}39.93)$ ppm for (DMSO), a single signal at $\delta(124)$ ppm for (C in imidazole ring), a single signal at $\delta(143)$ ppm for (CH of purine ring), a single signal at $\delta(150)$ ppm for (C-NH, in purine ring), a single signal at $\delta(159)$ ppm for (C=O, of purine ring), a single signal at $\delta(166)$ ppm, for (C-NH, in purine ring), a single signal at $\delta(176)$ ppm, for(C=O, amide), and a single signal at $\delta(184)$ ppm, for (C=S), **Table 3**.

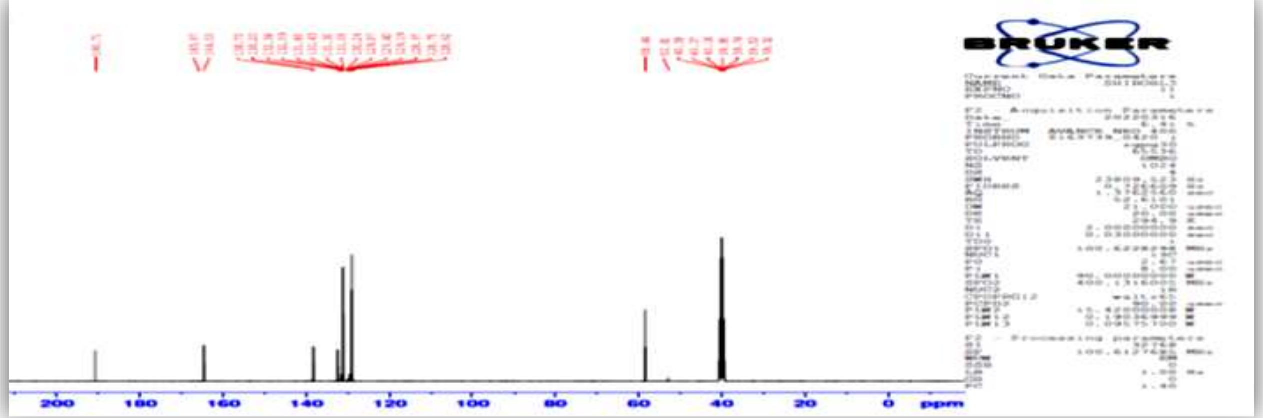

Figure 3. The ^{13}C-NMR spectrum of ligand (OPP).

Table 4. The ^{13}CNMR signals for ligand (OPP).

Symbol	Δppm	Group
a	10.23	CH_3,Methyl
b	30.02	CH_2,Methylene
c	124	C- imidazole ring
d	143	CH in purine ring
e	150	C-NH in purine ring
f	159	C=O in purine ring
g	166	C-NH in purine ring
h	176	C=O, amid
i	184	C=S

According to **Figure 5**, the UV-visible spectra of the ligand OPP (0.01M in DMSO) in **Table 4** displayed a band at (36101) cm^{-1}, which was attributed to the $\pi\rightarrow\pi^*$ transition, while a band at (27777) cm^{-1} was observed due to the $n\rightarrow\pi^*$ transitions [23].

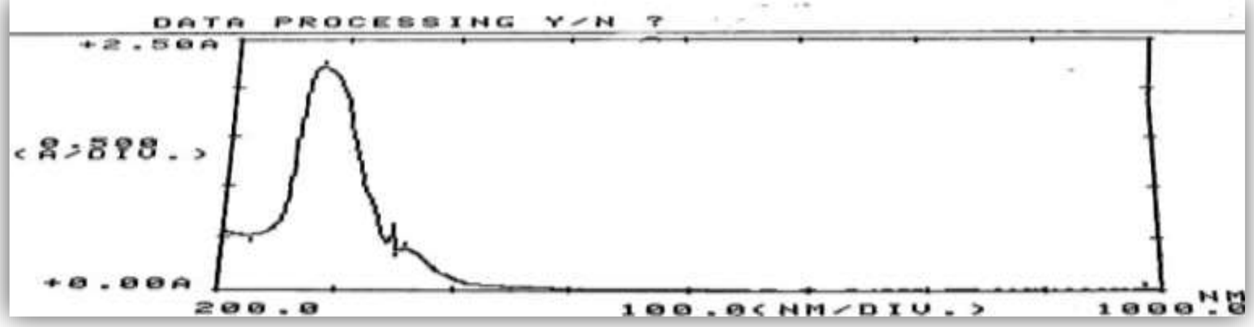

Figure 5. The UV-visible spectrum of ligand (OPP).

-$[MnCl_2(OPP)_2]$ d^5, displayed distinct spectral bands at (35087), (28735), and (10183) cm^{-1} were due to (L.F.) transitions, (C.T.), and $(^6A_1g \rightarrow {}^4T_{1(G)})$ transitions, respectively [19,23].

-$[CoCl_2(OPP)_2]$ d^7 in **Figure 6**, exhibited clear spectral bands at (34482), (28735), (34482), and (14836) cm^{-1}, which were associated with (L.F.), and (C.T.) that mix with $(^4T_{1(f)} \rightarrow {}^4T_{1(p)})$ transitions, $(^4T_1g_{(f)} \rightarrow {}^4A_2g)$ transitions, and $(^4T_1g_{(f)} \rightarrow {}^4T_2g)$ transitions, respectively [24,25].

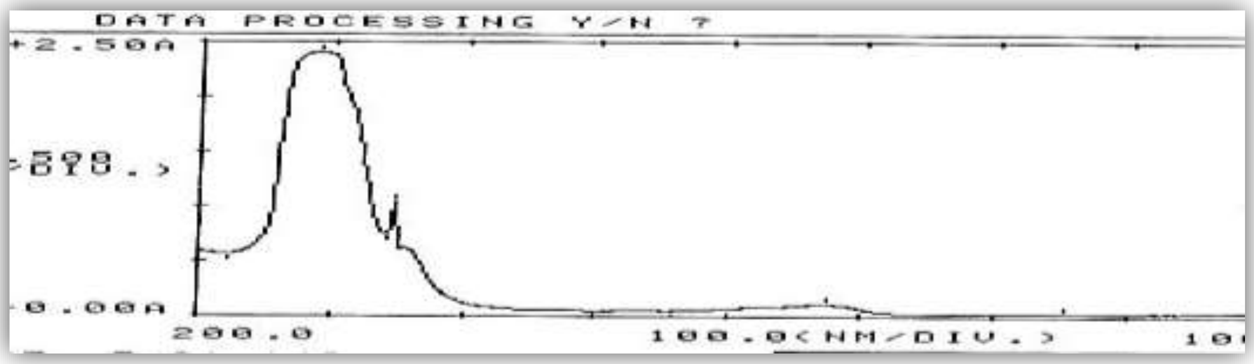

Figure 6. The UV-visible spectrum of $[CoCl_2(OPP)_2]$.

-$[NiCl_2(OPP)_2]$ d^8, the complex exhibited distinct spectral bands at (34013, 28735, 15197) and (11299) cm^{-1}, which were for ligand field (LF), charge transfer (CT) that mix with $(^3A_1g \rightarrow {}^3T_1g_{(p)})$, $(^3A_2g \rightarrow {}^3T_1g)$, and $(^3A_2g \rightarrow {}^3T_2g)$ transitions, respectively [24,25].

-$[PdCl_2(OPP)_2]$ d^8 in **Figure 10**, the complex exhibited distinct spectral bands at (34013, 28735,15197), and 11299) cm^{-1}, which were assigned for (L.F.), (C.T.) that mix with the $(^3A_1g \rightarrow {}^3T_1g_{(p)})$, $(^3A_2 \rightarrow {}^3T_1g)$, and $(^3A_2g \rightarrow {}^3T_2g)$ transitions, respectively [24,25].

-$[CuCl_2(OPP)_2]$ d^9 in **Figure 7**, displayed distinct spectral bands at (35087 and 10593) cm^{-1} which were attributed to (L.F.) and $(^2Eg \rightarrow {}^2T_2g)$ transitions, respectively [23].

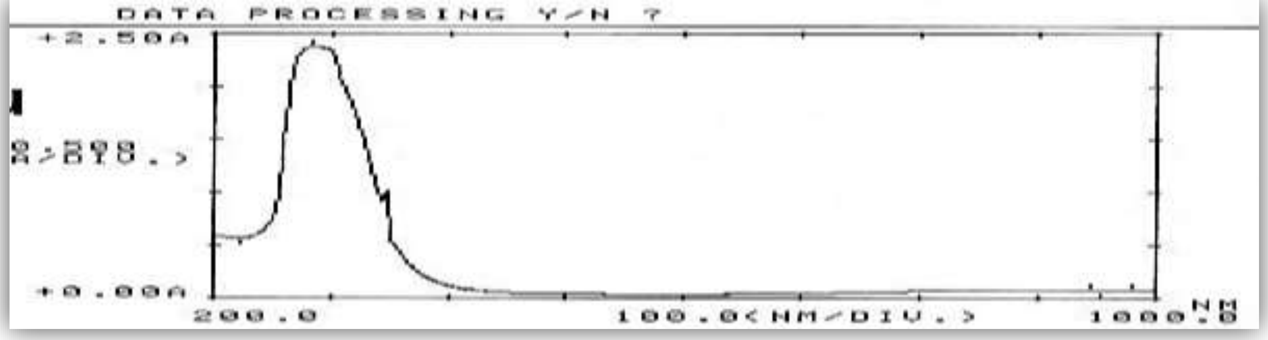

Figure 7. The UV-visible spectrum of $[CuCl_2(OPP)_2]$.

The complexes of $[ZnCl_2(OPP)_2]$ and $[CdCl_2(OPP)_2]$ in **Figures 12** and **13**, respectively, showed ligand field effects in the range (34129-34013) cm^{-1} and charge transfer of (M → L), in the range (29735-28735) cm^{-1} [24].

Table 5. The UV-visible spectral data of the ligand OPP complexes and its complexes (10^{-3} M in DMSO).

Compounds	**λ(nm)**	**υ^{-}(cm^{-1})**	**ABC**	**ε_{max} molar-^{1}cm^{-1}**	**Transitions**
(OPP)	277	36101	2.213	2213	$\pi \rightarrow \pi^*$
	360	27777	0.383	383	$n \rightarrow \pi^*$
[MnCl$_2$(OPP)$_2$]	285	35087	2.366	2366	(L.F.)
	348	28735	0.837	837	(C.T)
	982	10183	0.025	25	$^6A_1g \rightarrow {}^4T_{1(G)}$
[CoCl$_2$(OPP)$_2$]	290	34482	2.399	2399	(L.F.)
	348	28735	1.050	1050	(C.T.)mix $^4T_{1(f)} \rightarrow {}^4T_{1(p)}$
	678	14836	0.110	110	$^4T_1g_{(f)} \longrightarrow {}^4A_2g$
	870	34482	0.035	35	$^4T_1g_{(f)} \longrightarrow {}^4T_2g$
[NiCl$_2$(OPP)$_2$]	294	34013	2.416	2416	(L.F.)
	348	28735	1.169	1169	(C.T.)mix $^3A_1g \rightarrow {}^3T_1g_{(p)}$
	658	15197	0.036	36	$^3A_2g \rightarrow {}^3T_1g$
	885	11299	0.035	35	$^3A_2g \rightarrow {}^3T_2g$
[CuCl$_2$(OPP)$_2$]	285	35087	2.369	2369	(L.F.)
	944	10593	0.078	78	$^2Eg \rightarrow {}^2T_2g$
[ZnCl$_2$(OPP)$_2$]	294	34013	2.442	2442	(L.F.)
	348	28735	1.266	1266	(C.T.)
[CdCl$_2$(OPP)$_2$]	293	34129	2.383	2383	(L.F.)
	348	29735	1.050	1050	(C.T.)
[PdCl$_2$(OPP)$_2$]	273	36630	1.628	1628	(L.F.)
	352	28409	0.552	552	(C.T.)mix $^3A_2g \rightarrow {}^3T_1g_{(p)}$
	982	10183	0.069	69	$^3A_2g \rightarrow {}^3T_2g$

The FT-IR spectra of seven prepared complexes were recorded within the range (4000-200) cm^{-1} as (CsI) discs and showed significant differences in the bands associated with the stretching vibration at 1226 cm^{-1} in the ligand spectrum, which is assigned to the ν(C=S) in the range of (1182-1159) cm^{-1}. These bands were shifted lower by (44-23) cm^{-1} in the spectra of the complexes, indicating the involvement of the sulfur atom in the thione group in coordination [26], **Table 5**. The band caused by ν(C=O amide) in the range of (1595-1525) cm^{-1} was shifted to lower frequencies by (79-9) cm^{-1}, suggesting the possibility of coordination of the ligand through the O-atom at the carbonyl group the metal complexes [27,28] as in **Figures 8** and **9**. The coordination of M-O and M-S was evidenced by the appearance of stretching vibrations at around (487-455) cm^{-1}, (379-308) cm^{-1}, and (293-262) cm^{-1}, respectively, which correspond to υ(M-O), υ(M-S), and υ(M-Cl), [29]. **Table 6** describes the critical bands and their assignments for the free ligand (OPP) and its complexes that were prepared.

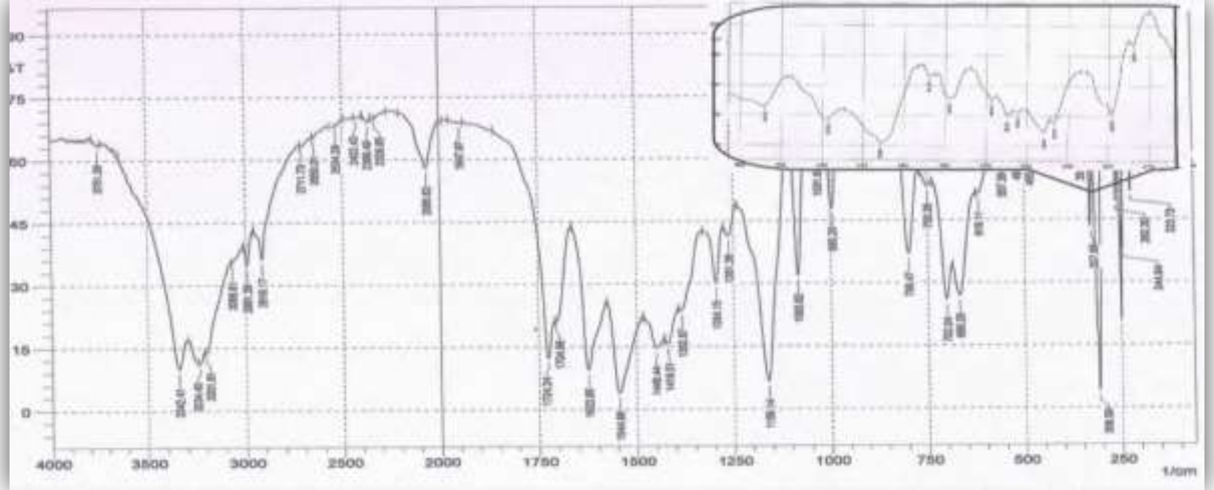

Figure 8. The FT-IR spectrum of [$CdCl_2(OPP)_2$] complexes.

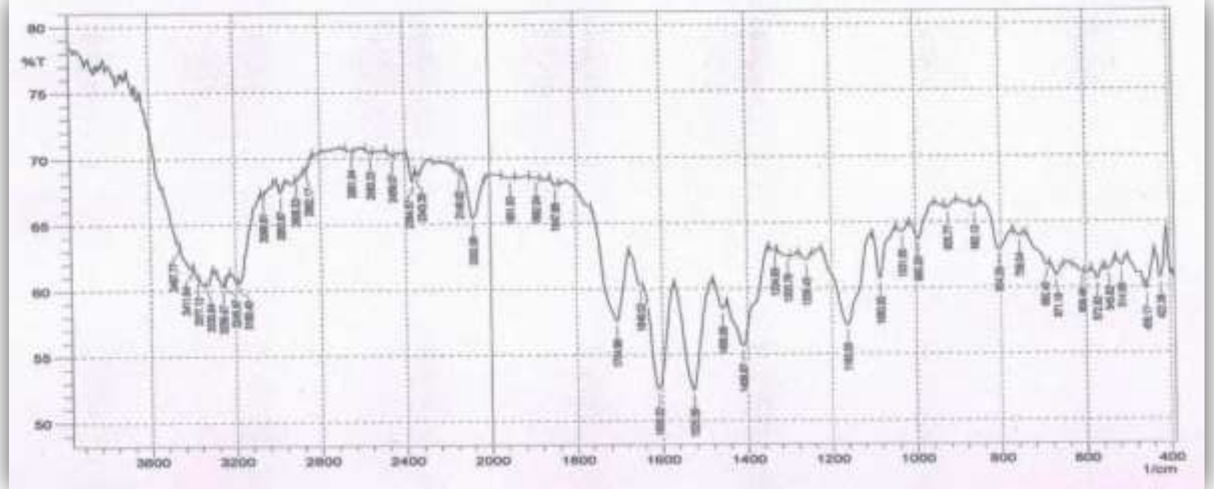

Figure 9. The FT-IR spectrum of [$ZnCl_2(OPP)_2$] complexes.

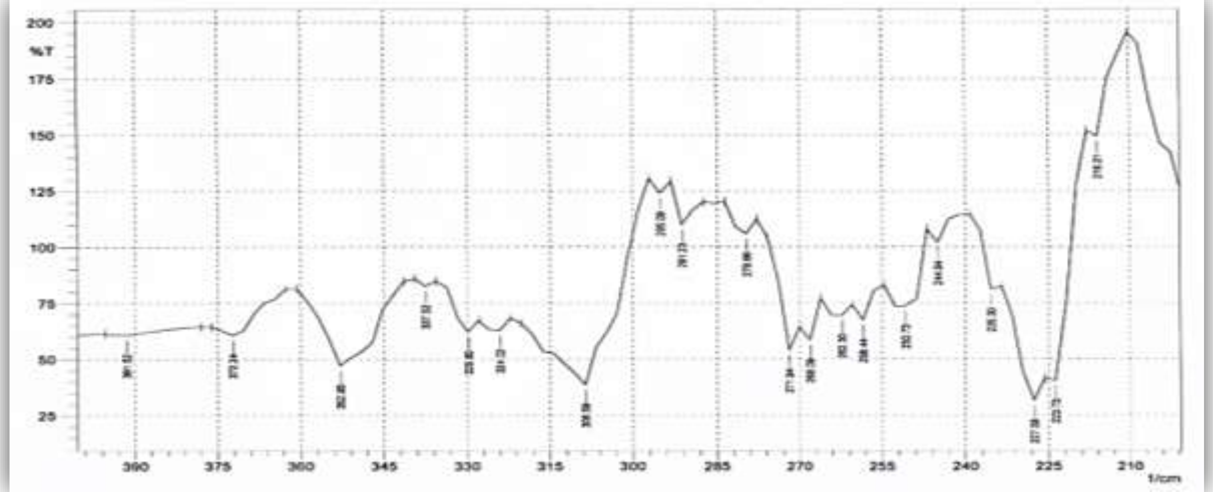

Figure 10. The FT-IR spectrum of [$ZnCl_2(OPP)_2$] complexes.

Table 6. The important bands and assignment for (OPP) and its metal complexes.

Compound	ν(N-H)	ν(C=O) Amide	ν(C=S)	ν(M-O)	ν(M-S)	ν(M-Cl)
Ligand (OPP)	3160$_{(m)}$	1604$_{(m)}$	1226$_{(m)}$	-----	-----	-----
$[MnCl_2(OPP)_2]$	3163$_{(m)}$	1593$_{(s)}$	1159$_{(s)}$	480$_{(w)}$	379$_{(w)}$	293$_{(w)}$
$[CoCl_2(OPP)_2]$	3170$_{(m)}$	1527$_{(s)}$	1180$_{(s)}$	462$_{(w)}$	329$_{(w)}$	268$_{(w)}$
$[NiCl_2(OPP)_2]$	3170$_{(m)}$	1595$_{(s)}$	1182$_{(s)}$	480$_{(w)}$	312$_{(w)}$	264$_{(w)}$
$[CuCl_2(OPP)_2]$	3178$_{(m)}$	1529$_{(m)}$	1161$_{(m)}$	487$_{(w)}$	310$_{(w)}$	270$_{(w)}$
$[ZnCl_2(OPP)_2]$	3180$_{(m)}$	1525$_{(m)}$	1163$_{(m)}$	455$_{(w)}$	308$_{(w)}$	271$_{(w)}$
$[CdCl_2(OPP)_2]$	3150$_{(m)}$	1544$_{(s)}$	1159$_{(s)}$	455$_{(w)}$	351$_{(w)}$	262$_{(w)}$
$[PdCl_2(OPP)_2]$	3166$_{(m)}$	1535$_{(m)}$	1161 $_{(s)}$	462$_{(m)}$	351$_{(w)}$	258$_{(w)}$

The magnetic susceptibilities of these complexes were in good agreement with the values expected for high spin [29,30]; the magnetic susceptibilities of these complexes are listed in **Table 7**.

Table 7. Magnetic susceptibilities data of (OPP) complexes.

Complexes	Gram susce. X_g x 10^{-6}	Molar susce. X_M x 10^{-6}	Atomic susce. X_A x 10^{-6}	μ_{eff} (B.M)	No. of unpaired electrons	Proposed structure
$[MnCl_2(OPP)_2]$	22.46	1478.4394	14787.4394	5.96	5	Oh
$[CoCl_2(OPP)_2]$	14.35	9506.7315	9631.9115	4.79	3	Oh
$[NiCl_2(OPP)_2]$	5.41	3582.8807	3708.0607	2.97	2	Oh
$[CuCl_2(OPP)_2]$	1.66	1107.22	1232.4	1.71	1	Oh
$[ZnCl_2(OPP)_2]$	0	0	0	0	0	Oh
$[CdCl_2(OPP)_2]$	0	0	0	0	0	Oh
D = 125.18×10^{-6}						

Based on molar conductivity, magnetic moment, and spectroscopic studies (including FT-IR, UV-Vis, ^{1}H-^{13}C NMR, and atomic absorption), this study determines that the ligand OPP acts as a bidentate ligand when coordinating with Mn(II), Co(II), Ni(II), Cu(II), Zn(II), Cd(II), and Pd(II) ions. Specifically, the oxygen atom of the amido group (C=O) and the sulfur atom of the thioamide group (C=S) are involved in coordination with the metal ion. This suggests an octahedral geometry around the metal ion for all of the prepared complexes, **Scheme 2**. Additionally, FT-IR studies for the OPP ligand show that it is coordinates with the mentioned functional groups.

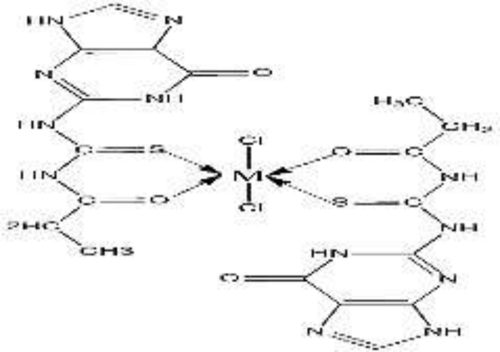

Scheme 2. Octahedral geometry of complexes.

4. Conclusion

This study utilizes a variety of analytical techniques to determine that the OPP ligand acts as a bidentate ligand when coordinating with Mn(II), Co(II), Ni(II), Cu(II), Zn(II), Cd(II), and Pd(II) ions. The amido group's oxygen atom (C=O) and the thioamide group's sulfur atom (C=S) coordinated with the metal ion, resulting in an octahedral geometry around the metal ion for all prepared complexes, as shown in **Scheme 2**. Furthermore, the OPP ligand showed that coordination occurred through the mentioned functional groups and the formation of hexagonal rings between the ligands and metal ions, which increased the stability of these complexes. In summary, this study provides comprehensive insights into the coordination behavior of the OPP ligand with various metal ions. It offers a detailed understanding of the structures of the prepared complexes using multiple analytical techniques.

Acknowledgment

The authors thank all those who contributed to the completion of this research project. First and foremost, they extend their heartfelt appreciation to Basima Muhsen Sarhan and Vishwa Deepak Tripathi for their invaluable guidance, encouragement, and expertise throughout this research. Their insightful feedback and unwavering support were instrumental in shaping the direction of this work. They also thank their colleagues and collaborators for their assistance and valuable discussions, which significantly contributed to the development and refinement of their ideas. Lastly, the authors would like to acknowledge the anonymous reviewers, whose constructive feedback and suggestions helped strengthen the manuscript.

Conflict of Interest

The authors declare that they have no conflicts of interest.

Funding

There is no financial support.

Ethical Clearance

This work has been approved by the Scientific Committee at the University of Baghdad/ College of Education for Pure Science (Ibn Al-Haiham).

References

1. Berg, J.M. Principles of bioinorganic chemistry, *University Science Books,Mill valley, California*, **1994**; pp. 1–6. https://iubmb.onlinelibrary.wiley.com/doi/pdf/10.1016/0307-4412%2895%2990685-1
2. Li, C.; Krautler, B. Transition metal complexes of phyllobilins- a new realm of bioinorganic chemistry. *Dalt Trans* **2015**, *44(22)*,10116–10127. https://doi: 10.1039/C5DT00474H.
3. Bagchi, A.N.; Mukherjee, P.R.; Raha, A.N. A review on transition metal complex-mordern weapon in medicine. *Int J Recent Adv Pharm Res* **2015**, *5*,171-180.
4. Hunsaker, E.W.; Franz, K.J. Emerging opportunities to manipulate metal trafficking for therapeutic benefit. *Inorg Chem* **2019**, *58(20)*,13528–13545. https://doi.org/10.1021/acs.inorgchem.9b01029.
5. Spencer, J.; Read, J.; Sessions, R.B.; Howell, S.; Blackburn, G.M.;Gamblin, S.J. Antibiotic recognition by binuclear metallo-β-lactamases revealed by x-ray crystallography. *J Am Chem Soc* **2005**, *127(41)*,14439–14444. https://doi.org/10.1021/ja0536062.
6. Andreini,C.;Bertini, I.;Cavallaro, G.; Holliday, G.L.; Thornton, J.M.Metal ions in biological catalysis From enzyme databases to general principles. *J Biol Inorg Chem* **2008**, *13(8)*,1205–1218.

https://link.springer.com/article/10.1007/s00775-008-0404-5#article-info.

7. Tanaka, Y. ; Nakagawa, N.; Kuramitsu, S.;Yokoyama, S.; Masui, R. Novel reaction mechanism of GTP cyclohydrolase I. High-resolution X-ray crystallography of thermus thermophilus HB8 enzyme complexed with a transition state analogue, the 8-oxoguanine derivative. *J Biochem* **2005**, *138(3)*, 263–275. https://doi.org/10.1093/jb/mvi120.
8. Orts-Arroyo, M.; Gutiérrez, F.; Gil-Tebar, A.; Ibarrola-Villava, M.; Jiménez-Martí, E.; Silvestre-Llora, A.; Castro, I.; Ribas, G.; Martínez-Lillo, J. A novel adenine-based diruthenium (III) complex synthesis, crystal structure, electrochemical properties and evaluation of the anticancer activity. *Journal of Inorganic Biochemistry* **2022**, *1(232)*,111812. https://doi.org/10.1093/jb/mvi120.
9. Li, Y.; Dong, J.; Zhao, P.;Hu, P.; Yang, D.; Gao, L.; Li, L. Synthesis of amino acid schiff base nickel (II) complexes as potential anticancer drugs in vitro. *Bioinorg Chem Appl* **2020**, *2020*, 8834859. https://doi: 10.1155/2020/8834859.
10. Szymańska, M.; Pospieszna-Markiewicz, I.; Mańka, M.; Insińska-Rak ,M.; Dutkiewicz, G.; Patroniak, V.; Fik-Jaskółka, M.A. Synthesis and spectroscopic investigations of schiff base ligand and its bimetallic Ag (I) complex as DNA and BSA binders. *Biomolecules* **2021**, *11(10)*,1449. https://doi.org/10.3390/biom11101449.
11. Chen, C.K.J.; Hambley ,T.W. The impact of highly electron withdrawing carboxylato ligands on the stability and activity of platinum(IV) pro-drugs. *Inorganica Chim Acta* **2019**, *1(494)*,84–90. https://doi.org/10.1016/j.ica.2019.05.001.
12. Skalnaya, M.G.; Skalny, A.V. Essential trace elements in human health, *a physician's view. Tomsk, Publishing House of Tomsk State University* **2018**; *S66*, pp. 224. https://trace-element.org/sites/default/files/2022-02/essential-trace-elements-in-human-health-a-physician-s-view_124_fr_0.pdf.
13. Correa, R.S.; Bomfim, L.M.; Oliveira, K.M.; Moreira, D.R.M.; Soares, M.B.P.; Ellena, J.; Daniel, P.; Bezerra, A.A.B. Ru(II) complexes containing uracil nucleobase analogs with cytotoxicity against tumor cells. *J Inorg Biochem* **2019**, *198(2)*,110751. https://en.trace-element.org/sites/default/files/2022-02/essential-trace-elements-in-human-health-a-physician-s-view_124_fr_0.pdf.
14. Sherin, D.; Manojkumar, T.K. Exploring the selectivity of guanine scaffold in anticancer drug development by computational repurposing approach. *Sci Rep* **2021**, *11(16251)*,1-11. https://doi:10.1038/s41598-021-95507-4.
15. Marotta, C.; Giorgi, E.; Binacchi, F.; Cirri, D.; Gabbiani, C.; Pratesi, A. An overview of recent advancements in anticancer Pt(IV) prodrugs: New smart drug combinations, activation and delivery strategies. *Inorganica Chim Acta* **2023**, *548(121388)*,1-26. https://doi:10.1016/j.ica.2023.121388.
16. Jaber, S.S.; Sarhan, B.M. Synthesis and characterization of some new matals complexes of (propionyl carbamothioyl) valine (PCV). *Pakistan J Med Heal Sci* **2022**, *16(4)*,420–423. https://doi.org/10.53350/pjmhs22164420.
17. Kader, T.A.; Sarhan, B.M. Synthesis and spectroscopic study of new ligand 3-(acetylthioureido) propanoic acid with their metal complexes. *Int J Health Sci Qassim* **2022**, *6(S2)*,11716–11728. https://doi:10.53730/ijhs.v6nS2.8128.
18. Alwan, T.B.; Sarhan, B.M. Synthesis and characterization of some metal complexes of [1-(4-bromo-2-methyl-phenyl)-3-(4-methoxybenzoyl)-thiourea. *J Glob Pharma Technol* **2018**, *10(8)*,42–50. https://www.researchgate.net/publication/355486493_Synthesis_and_Characterization_of_Some_Metal_Complexes_of_1-4-_Bromo-2-Methyl-Phenyl-3-4-Methoxybenzoyl-Thiourea.
19. Kindeel, A.S. Synthesis and characterization of new metals complexes of [N- (acetyl amino) thioxomethyl] valine. *Ibn Al-Haitham J Pure Appl Sci* **2013**, *26(1)*,225–233. https://www.iasj.net/iasj/download/4a4ca1072da6558d.
20. Uchida, K.; Toyama, A.; Tamura, Y.; Sugimura, M.; Mitsumori , F.; Furukawa, Y.; Takeuchi, H.; Harada, I. Interactions of guanine derivatives with ethylenediamine and diethylenetriamine

complexes of palladium(II) in solution: Pd binding sites of the guanine ring and formation of a cyclic adduct, [{Pd(en) (guanine ring)}4]. *Inorg Chem* **1989**, *28(11)*,2067–2073. https://doi.org/10.1021/ic00310a012.

21. Fayyadh, B.M.; Jaafar, W.A.; Sarhan, B.M. Synthesis, structural study, and biological activity evaluation of Vo(II), Mn(II), Co(II), Ni(II), Cu(II), Zn(II), Cd(II), and Hg(II) complexes with new schiff base ligand derived from pyrazine. *International Journal of Drug Delivery Technologythis* **2021**, *11(1)*,64–69. https://doi: 10.25258/ijddt.11.1.11.
22. Chennakrishnan, S.; Ravi Kumar, S.M.; Shanthi, C.; Srineevasan, R.; Kubendiran, T.; Sivavishnu, D.; Packiya raj, M. Synthesis of the semi-organic nonlinear optical crystal l-glutamic acid zinc chloride and investigation of its growth and physiochemical properties. *J Taibah Univ Sci* **2017**, *11(6)*, 955–965. https://doi.org/10.1016/j.jtusci.2017.01.001.
23. Sarhan, B.M.; Abed, A.H.; Rumez, R.M. Synthesis and characterization of some mixed ligand complexes containing (8-hydroxyquinoline) and (2- picoline) with some metal Ions. *Baghdad Sci J* **2013**, *10(2)*,396–404. https://www.iasj.net/iasj/download/f1ef85c3b330c698.
24. Gastaca, B.; Galletti, G.; Sánchez, H.R.; Diez, R.P.; Schiavoni, M.M.; Furlong, J.J.P. GC/MS Analyses of thiosemicarbazones synthesized from acetophenones: Thermal decay and mass spectra features. *Int J Anal Mass Spectrom Chromatogr* **2015**, *3(1)*,1-13. https://doi: 10.4236/ijamsc.2015.31001.
25. Prokopchuk, E.D.; Sonnenberg, F.J.; Meyer, N.; Zimmer-De Iuliis, M.; Lough, J.A.; Morris, H.R. Spectroscopic and DFT study of ferraaziridine complexes formed in the transfer hydrogenation of acetophenone catalyzed using trans-[Fe(CO)(NCMe)(PPh$_2$C6H4CH═NCH$_2$−)$_2$-κ4P,N,N,P](BF$_4$)$_2$. *Organometallics* **2012**, *31(8)*, 3056–3064. https://doi.org/10.1021/om201170f.
26. Singh, V.P.; Katiyar, A. Synthesis, structural studies and bio-activity of Mn(II), Co(II), Ni(II), Cu(II) and Zn(II) complexes with p-amino acetophenone salicyloyl hydrazone. *J Coord Chem.* **2008**, *61(20)*, 3200–3212. https://doi.org/10.1080/00958970802017646.
27. Chandra, S.; Gupta, K. Twelve-, fourteen- and sixteen-membered macrocyclic ligands and a study of the effect of ring size on ligand field strength. *Transit Met Chem* **2002**, *27(2002)*,329–332. https://doi.org/10.1023/A:1014898706298.
28. Kadhim, M. A.; Sh. Abdullah Alani, A.; Hussein, N.M. Synthesis, characterization and biological evaluation of some phthalazine derivatives. *Materials Today: Proceedings* **2022**, *5772*. https://doi.org/10.1016/j.matpr.2021.04.156.
29. Al-Krboly, A.M.; M. Sarhan, B.; Alany, Sh.A. Synthesis and Characterization of new metals complexes of [N-(4- chlorobenzoylamino)-thioxomethyl]valine (cbv). *IOSR Journal of Applied Chemistry* **2014**, *7(11)*,67–73. https://doi.org/10.9790/5736-071116773.
30. Fayyadh, B.M.; Jaafar, W.A.; Sarhan, B.M. Synthesis, structural study, and biological activity evaluation of Vo(II), Mn(II), Co(II), Ni(II), Cu(II), Zn(II), Cd(II), and Hg(II) complexes with new schiff base ligand derived from pyrazine. *International Journal of Drug Delivery Technology* **2021**, *11(1)*,64–69. https://doi.org/10.25258/ijddt.11.1.11.